

Merging C–H Bond Activation, Alkyne Insertion, and Rearrangements by Rh(III)-Catalysis: Oxindole Synthesis from Nitroarenes and Alkynes

Marie Peng,[§] Chang-Sheng Wang,[§] Pan-Pan Chen,[§] Thierry Roisnel, Henri Doucet, K. N. Houk,^{*} and Jean-François Soule^{*}



Cite This: <https://doi.org/10.1021/jacs.2c10932>



Read Online

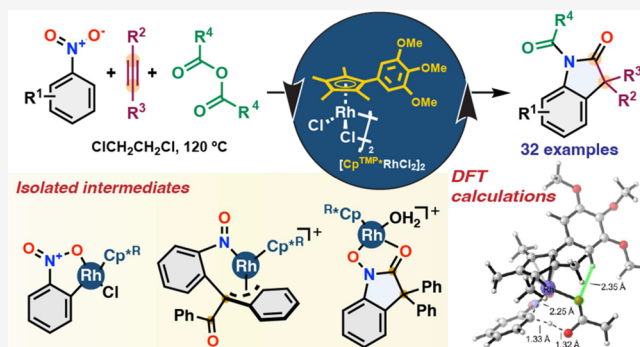
ACCESS |

Metrics & More

Article Recommendations

Supporting Information

ABSTRACT: We report a Rh(III)-catalyzed *ortho*-C–H bond functionalization of nitroarenes with 1,2-diarylalynes and carboxylic anhydrides. The reaction unpredictably affords 3,3-disubstituted oxindoles with the formal reduction of the nitro group under redox-neutral conditions. Besides good functional group tolerance, this transformation allows the preparation of oxindoles with a quaternary carbon stereocenter using nonsymmetrical 1,2-diarylalynes. This protocol is facilitated by the use of a functionalized cyclopentadienyl ($\text{Cp}^{\text{TMP}*}$)Rh(III) [$\text{Cp}^{\text{TMP}*} = 1-(3,4,5\text{-trimethoxyphenyl})-2,3,4,5\text{-tetramethylcyclopentadienyl}$] catalyst we developed, which combines an electron-rich character with an elliptical shape. Mechanistic investigations, including the isolation of three rhodacycle intermediates and extensive density functional theory calculations, indicate that the reaction proceeds through nitrosoarene intermediates via a cascade of C–H bond activation—O-atom transfer—[1,2]-aryl shift—deoxygenation—*N*-acylation.



INTRODUCTION

Nitrogen-containing heterocycles are essential to life science since they are abundant in nature and exist as subunits in several natural products and more than half of the prescribed drugs contain an *N*-heterocycle backbone.¹ Moreover, they have also found diverse applications in materials sciences.² Therefore, their formations, manipulations, and diversifications represent a significant stake for chemical companies, and the discovery of novel synthetic approaches fulfilling modern reaction ideals of green chemistry is still an important challenge, especially starting from low-functionalized materials. Since the pioneer studies by Fagnou on the Rh(III)-catalyzed C–H bond annulation of acetanilides with alkynes for the synthesis of indoles,³ several *N*-directed C–H bond annulation protocols have been developed for straightforward access to *N*-heterocycles.⁴ However, the conditions often required a stoichiometric amount of the oxidant. An external oxidant-free alternative consists of merging C–H bond functionalization with O-atom transfer (OAT)—proving that the directing group holds an *N*–O bond—then, the resulting intermediate can undergo rearrangements to roll *N*-heterocycles in a one-pot cascade process (Figure 1A). This strategy was initially reported by Li and co-workers using quinoline-*N*-oxides, albeit the reaction stopped after the OAT (Figure 1B).⁵ Shortly later, the $\text{Cp}^*\text{Rh(III)}$ -catalyzed one-pot cascade of C–H bond functionalization—OAT—rearrangement was implemented to

prepare indolyl scaffolds from aryl nitroles (Figure 1C),⁶ indoles from aryl nitroles (Figure 1D),⁷ or amine-*N*-oxides (Figure 1E).⁸ Although the high efficiency of these methods for the direct synthesis of *N*-heterocycles, all require the preinstallation of the oxidizing directing group (*N*–O bond) using hazardous reagents.⁹

Nitroarenes constitute abundant feedstocks of *N*-containing molecules as they are readily prepared by the nitration of arenes.¹⁰ Despite a few examples of C–H bond functionalizations of nitroarenes,¹¹ the NO_2 group has never been considered as a suitable oxidizing directing group to develop redox-neutral coupling reactions yet. Therefore, we plan to use nitroarenes in the $\text{Cp}^*\text{Rh(III)}$ -catalyzed one-pot cascade of C–H bond functionalization—OAT—rearrangement(s) (Figure 1F). The advantage of this approach is to employ naturally occurring NO_2 as an oxidizing directing group. Moreover, the OAT should deliver nitrosoarene intermediates, which are very reactive and undergo unpredictable rearrangements toward *N*-

Received: October 23, 2022

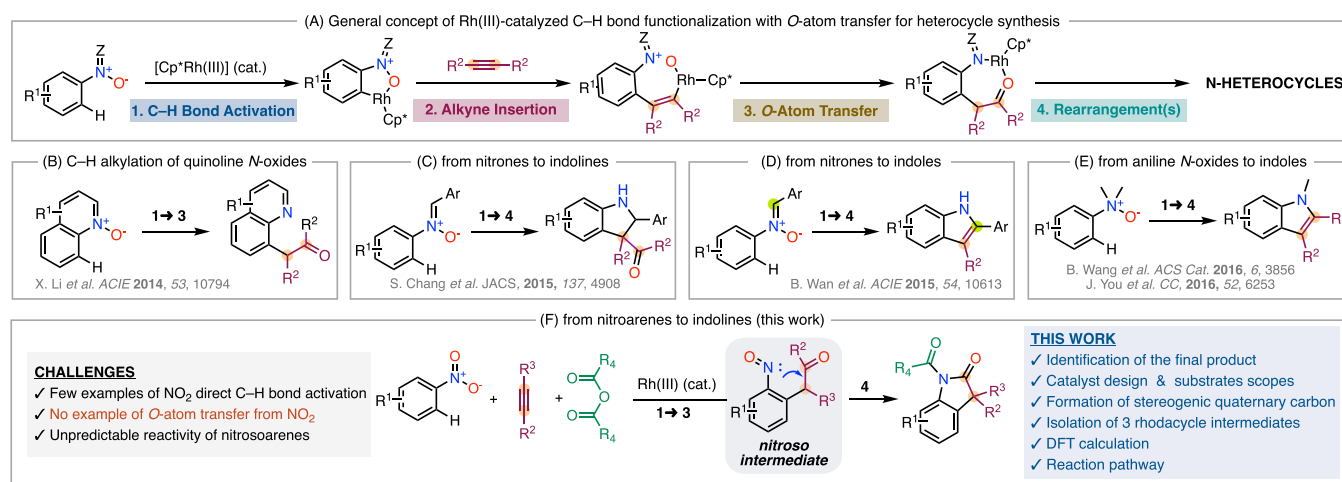


Figure 1. *N*-Heterocycle synthesis by Rh(III)-catalyzed C–H bond activation, alkyne insertion, OAT, and rearrangements.

heterocycles.¹² In contrast to previous methods to generate nitrosoarenes which employ reductants, our strategy is redox-neutral. This cascade approach led us to discover a novel synthesis of oxindoles. In retrospect to the realization of this unpredictable endeavor, we also optimized the catalyst design, investigated the scope of the reaction, and thoughtfully studied the reaction mechanism.

RESULTS AND DISCUSSION

Reaction Development. We began our studies on Rh-catalyzed C–H bond activation by reacting nitrobenzene with diphenylacetylene in the presence of [Cp^RRhCl₂]₂ in 1,2-dichloroethane at 120 °C. Surprisingly, we observed the unexpected formation of oxindole **1** in 41% yield that was formed upon *ortho*-C–H bond annulation of nitrobenzene via a multistep reaction: twofold reduction of NO₂, migration of alkyne phenyl group, and *N*-acylation (Table 1, entry 1). The structure of **1** was secured by X-ray analysis. This class of oxindoles containing an α-carbonyl quaternary center was widely recognized as valuable synthetic intermediates, forming the core of numerous natural products and drugs, often requiring several consecutive reactions.¹³ A solvent screen revealed 1,2-dichloroethane to be essential for the reaction outcomes, whereas most of the common additives employed in C–H bond functionalization had deleterious effects and did not suppress or decrease the oligomerization of alkyne as the side reaction.¹⁴ Following the seminal contributions of Rovis and co-workers,¹⁵ Shibata and Tanaka,¹⁶ and Cramer and co-workers¹⁷ on the modification of Cp ligands to improve the selectivity and performance in Rh(III) catalysis in other reactions, we decided to evaluate an array of [Cp^RRhCl₂]₂ catalyst precursors (Table 1). Electron-deficient [Cp^ERhCl₂]₂ was inactive for this transformation (Table 1, entry 2).¹⁸ The Rh(III) complex surrounded by the Cp^{iPr}* ligand, having a similar disc shape and electronic nature than Cp*,¹⁵ gave the desired product **1** in a similar yield (Table 1, entry 3). We next prepared a set of Rh(III) complexes holding C₅Me₄-Ar ligands exhibiting an elliptical shape. The presence of substituents at the *para* position on the aryl group affects the redox potentials predictably, decreasing in the order of [CF₃ (−1.21), H (−1.24), and OMe (−1.25)], which is consistent with an increase in electron density of the rhodium center. Increasing the electron density of the Cp ring resulted in an improvement of the yields [Cp^{TFT}*Rh (10%) < Cp^{Ph}*Rh (25%) < Cp^{MP}*Rh

Table 1. Optimization: Nature of the Cp-Ligand^a

disc-shape

[Cp^RRhCl₂]₂ (−1.34[#]) [Cp^ERhCl₂]₂ (−0.84[#]) [Cp^{iPr}*RhCl₂]₂ (−1.33[#])

= E(Rh^{III}/Rh^{II}) (V vs. Cp₂Fe)

elliptical-shape

Cp^{TFT}* (−1.21[#]) Cp^{Ph}* (−1.24[#]) Cp^{MP}* (−1.25[#]) Cp^{DMP}* (−1.25[#]) Cp^{TMP}* (−1.26[#])

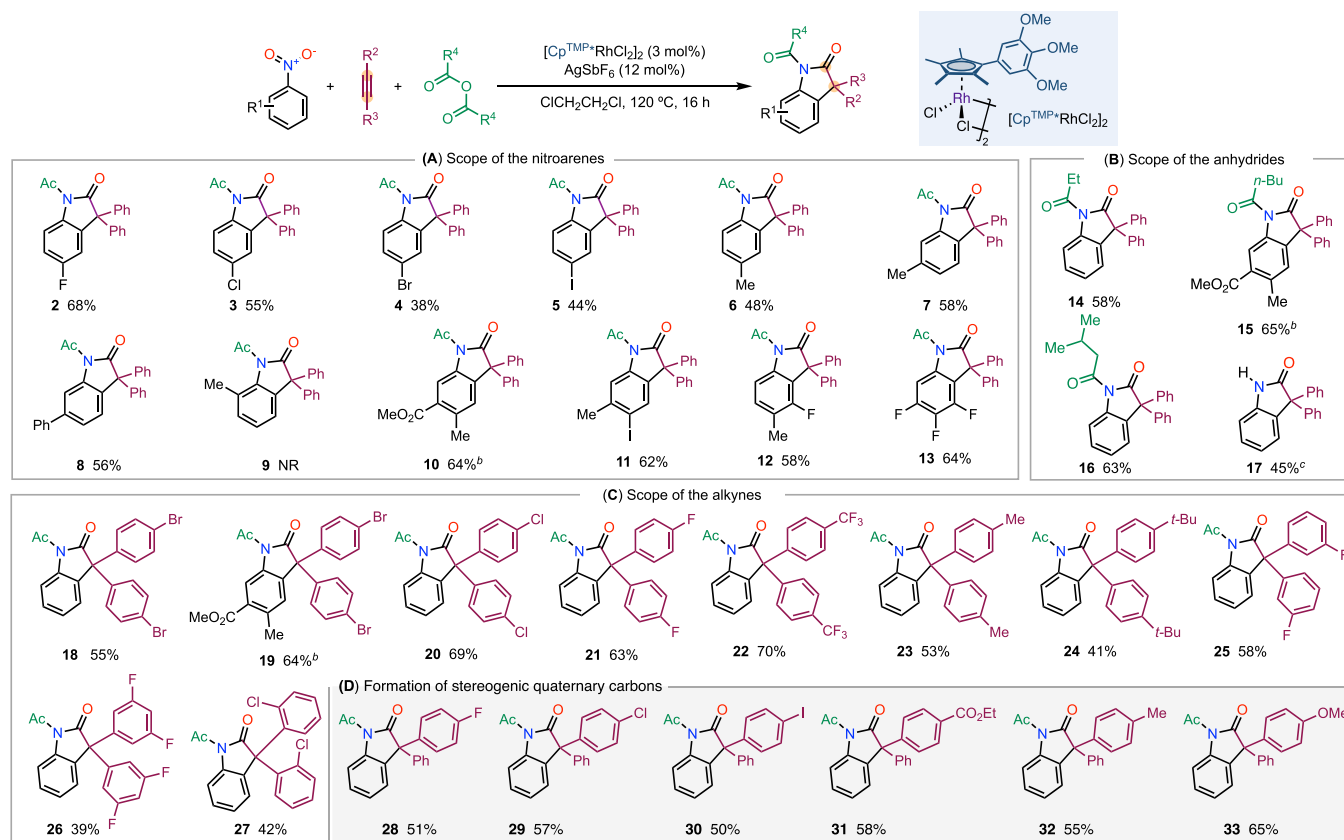
X-Ray structures

1 [Cp^{TFT}*RhCl₂]₂ [Cp^{TMP}*RhCl₂]₂

entry	[Cp ^R RhCl ₂] ₂	conv. (%) ^b	yield 1 (%) ^b
1	[Cp ^R RhCl ₂] ₂	100	41 ^c
2	[Cp ^E RhCl ₂] ₂	0	0 ^c
3	[Cp ^{iPr} *RhCl ₂] ₂	100	42 ^c
4	[Cp ^{TFT} *RhCl ₂] ₂	67	10 ^c
5	[Cp ^{Ph} *RhCl ₂] ₂	100	25 ^c
6	[Cp ^{MP} *RhCl ₂] ₂	100	55 ^c
7	[Cp ^{DMP} *RhCl ₂] ₂	100	64 ^c
8	[Cp ^{TMP} *RhCl ₂] ₂	100	79 (72%) ^c
9		0	0 ^c
10 ^d	[Cp ^{TMP} *RhCl ₂] ₂	100	45 ^c

^a[Cp^RRhCl₂]₂ (3 mol %), AgSbF₆ (12 mol %), nitrobenzene (5 mmol), diphenylacetylene (0.5 mmol), and acetic anhydride (2 mmol) in 1,2-dichloroethane (2 mL) at 120 °C. ^bDetermined by gas chromatography (GC)-analysis using *n*-dodecane as the internal standard, conversion is based on diphenylacetylene consumption; isolated yield is shown in parentheses. ^cAlkyne-oligomers are observed as side products by GC–mass spectrometry (MS) analysis. ^dNitrobenzene (2.5 mmol).

(55%)] (Table 1, entries 4–6). Subsequently, we prepared two novel [C₅Me₄-ArRhCl₂]₂ complexes with Ar = 3,4-dimethoxyphenyl (DMP) and 3,4,5-trimethoxyphenyl (TMP). Incorporation

Scheme 1. Scope of the Rh(III)-Catalyzed C–H Bond Activation with Migrations of Nitroarenes^a

^aNitroarene (5 mmol), diarylacetylene (0.5 mmol), and carboxylic anhydride (2 mmol), [Cp^{TMPP}*RhCl₂]₂ (3 mol %), AgSbF₆ (12 mol %), 1,2-dichloroethane (2 mL) at 120 °C, 16 h. ^bNitroarene (2.5 mmol). ^cUsing AcOH instead of Ac₂O.

rating additional methoxy substituents affects the electronic nature slightly, but their multiplication leads to a bulkier system. Both complexes displayed higher reactivity, and the best result was obtained with [Cp^{TMPP}*RhCl₂]₂, allowing the formation of **1** in 72% isolated yield (Table 1, entries 7 and 8). No reaction occurred without the Rh(III) catalyst (Entry 9). Similar to the C–H bond arylation of nitroarenes,^{11a} the use of a large excess of nitrobenzene (10 equivalents) is required (Entry 10), but most of the nitrobenzene (70–85%) can be recovered by distillation after the reaction.

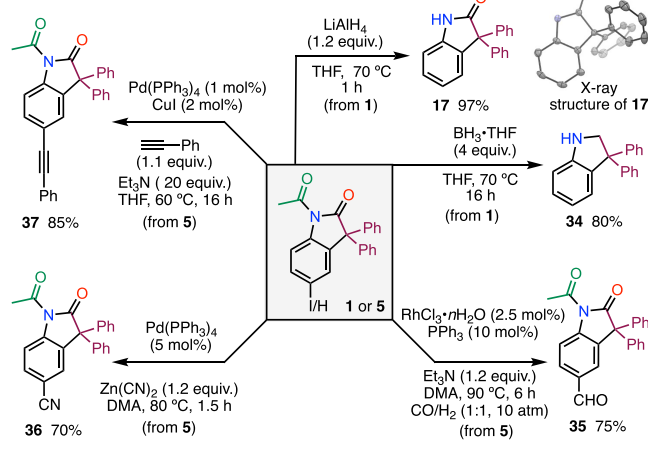
Scope of the Reaction. With the optimized conditions in hand using [Cp^{TMPP}*RhCl₂]₂, the scope of nitroarene, alkyne, and carboxylic anhydride partners was evaluated. We first subjected 12 different nitroarenes, adorned with various functional groups with different substitution patterns, to this C–H bond alkenylation – OAT – [1,2]-aryl shift – deoxygenation – *N*-acylation cascade reaction (Scheme 1A). Halides (i.e., F, Cl, Br, I) at the *para*-position of the nitro group were well tolerated and delivered the corresponding products in good to moderate yields (2–5). *Para*- or *meta*-nitrotoluene reacted to afford oxindoles **6** and **7** in 48 and 58% yield, respectively; while *ortho*-nitrotoluene did not react (**9**). The reaction was regioselective with *meta*-substituted nitroarenes (R = Me or Ph), affording the products resulting from activating the less hindered C6–H bond (**7**, **8**). From 5 equivalents of methyl 2-methyl-5-nitrobenzoate, the corresponding oxindole **10** was isolated in 64% yield. From disubstituted nitroarenes at *para* and *meta*-positions, the corresponding products were obtained in good yields as single

regioisomers (**11**, **12**). Interestingly, when the *meta* substituent is an F atom, the reaction occurs at its adjacent C–H bond (**12**). The electronically enhanced *ortho*-to-fluorine selectivity is a common feature observed in C–H bond functionalizations involving a concerted metalation-deprotonation (CMD) mechanism.¹⁹ Reaction with 3,4,5-trifluoronitrobenzene gave an excellent yield (**13**). Propionic, valeric, and isovaleric anhydrides gave the corresponding products in good yields (**14**–**16**) (Scheme 1B). The use of AcOH instead of Ac₂O affords the NH-free oxindole **17** in 45% yield. A broad range of 1,2-diaryl alkynes was readily converted to the corresponding oxindole products in modest to good yields (Scheme 1C). The reaction conditions were compatible with a variety of functional groups at the *para*-position, such as bromo (**18**, **19**), chloro (**20**), fluoro (**21**), trifluoromethyl (**22**), and alkyl (**23**, **24**). The reaction outcomes were not affected by the substitution patterns of the aryl group as a fluorine-atom at the *meta*-position (**25**, **26**) or a chlorine-atom at the *ortho*-position (**27**) were well tolerated. It should be noted that the [1,2]-aryl shift took place with complete retention of the regioselectivity of the migrated aryl group. We next explored this transformation with 1,2-diaryl alkynes containing two different aryl groups to form oxindoles with an α -carbonyl quaternary stereogenic center (Scheme 1D). Again, the reaction tolerated a wide range of functional groups such as F, Cl, I, CO₂Et, Me, and OMe affording the oxindoles **28**–**33** in 50–65% yields. However, no reaction occurred with dialkyl alkynes or alkyl aryl alkynes, as we have observed the both starting materials.

This lack of reactivity might be due to a change of an aryl group by an alkyl group that prevents the [1,2]-aryl shift step.

Postfunctionalizations. In addition, to further illustrate the synthetic value of this novel reaction, we investigated the reduction of amide groups (Scheme 2). In the presence of

Scheme 2. Access to Molecular Diversity through Postfunctionalizations



LiAlH_4 , the selective reduction of the acetyl group was observed, affording the indolin-2-one **17** in 97% yield, while compound **1** was fully reduced using borane–tetrahydrofuran to deliver **34** in 80% yield. These 3,3-disubstituted indolines—which are architectures embedded in many complex alkaloids or key building blocks—are now easy to prepare from nitrobenzene in only two steps, where formerly multistep synthesis was necessary.²⁰ Due to the strongly electron-withdrawing nature of the nitro group, the main limitation of our novel cascade reaction is incompatibility with electron-poor nitroarenes because of an unfavorable C–H bond activation.¹¹ To improve the diversity of structures accessible through this methodology, we performed several postfunctionalizations of iodo-substituted oxindoles. First, a formyl group was introduced through Rh(III)-catalyzed hydroformylation, affording oxindole **35** in 75% yield. Pd-catalyzed cyanation with $\text{Zn}(\text{CN})_2$ as a coupling reagent allowed to prepare 5-nitrile-substituted oxindole **36** in 70% yield. Finally, we also succeeded in preparing alkynyl-substituted oxindole **37** through the Pd/Cu-catalyzed Sonogashira reaction with phenylacetylene in 85% yield.

Experimental Mechanistic Investigations. In order to get insight into this unpredictable reaction, mechanistic experiments were conducted (Figure 2).²¹ Significant kinetic isotope effects (KIE 3.5 or 2.6) with both $[\text{Cp}^{\text{TMP}}*\text{RhCl}_2]_2$ and $[\text{Cp}^*\text{RhCl}_2]$ support that the C–H bond cleavage corresponds to the turnover determining step of the catalytic cycle (Figure 2A). Next, we decided to map the reaction by capturing potential rhodacycles and studying their reactivity (Figure 2B). Our attempts to isolate a cyclometalated Rh(III) intermediate from a stoichiometric reaction between nitrobenzene and $[\text{Cp}^{\text{TMP}}*\text{RhCl}_2]_2$ in the presence or absence of AgSbF_6 and acetate sources failed. However, cyclometalated Rh(III) **38a** has been prepared by transmetalation from 2-nitrophenylmercurial.²² The reaction between **38a** and 1-diphenylacetylene with AgSbF_6 in 1,2-dichloroethane at room temperature (RT) afforded Rh(III) η^3 -benzyl complex **39a**. This $18e^-$ complex **39a** was fully characterized by nuclear

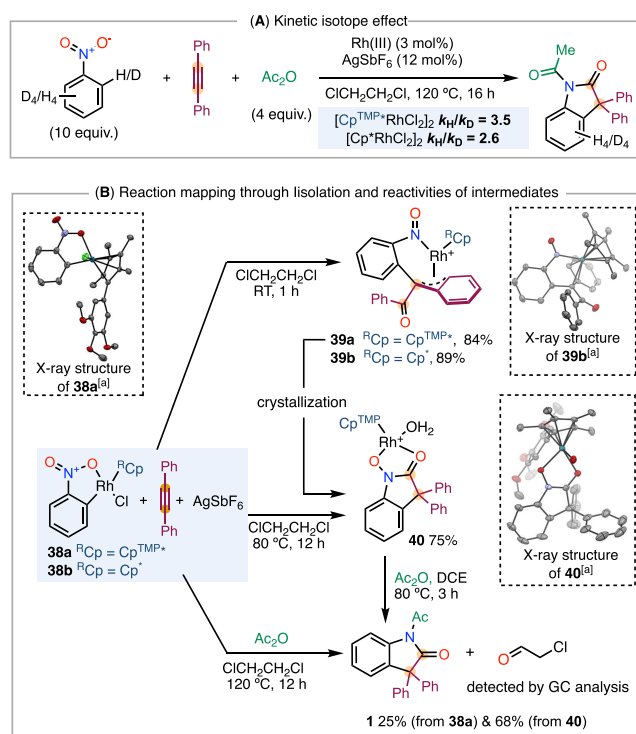


Figure 2. Determination of the mechanism. (a) Hydrogen atoms and SbF_6^- are omitted for clarity. Thermal ellipsoids are at the 50% probability level. $[\text{Cp}^{\text{TMP}}*\text{Rh}^+] = [\text{Cp}^{\text{TMP}}*\text{Rh}^+](\text{SbF}_6^-)$, $[\text{Cp}^*\text{Rh}^+] = [\text{Cp}^*\text{Rh}^+](\text{SbF}_6^-)$.

magnetic resonance (NMR) spectroscopy, mainly, the exchange η^3 -benzyl unit was observed by nuclear Overhauser effect spectroscopy experiments.¹⁴ This intermediate **39a** results from the alkyne insertion into Rh–C bond followed by OAT. We tried to get some crystal for X-ray analysis, but **39a** spontaneously evolved into **40**. We, therefore, repeated the experiments with $[\text{Cp}^*\text{RhCl}_2]_2$. Successfully, the Rh(III) η^3 -benzyl complex **39b** was obtained as single crystals and analyzed by X-ray experiments, demonstrating that OAT has proceeded to give the formal hydration of alkyne among with coordinated nitrosobenzene. When this reaction was conducted at 80 °C, Rh(III) complex **40** was isolated by crystallization in good yield and was fully characterized, including by X-ray structure. This intermediate **40** is formed via the N–Rh bond insertion into the carbonyl group followed by a migration of the phenyl ring at the *meso*-position of the nitrobenzene ring. Finally, the reaction from **38a** or **40** in the presence of Ac_2O at 120 °C furnished the desired product **1**. Combining with the detection of 2-chloroacetaldehyde by GC-analysis, these results suggest that the second N–O bond cleavage occurred through O-alkylation with 1,2-dichloroethane followed by a hydride-shift (Scheme S11 and Figures S24–26).²³ In addition, it should be mentioned that all isolated Rh(III)-complexes (**38a**, **39a**, and **40**) catalyze the reaction indicating they are intermediates of the reaction (Table S5).¹⁴

Theoretical Mechanistic Investigations. The experimental investigations outlined above have elucidated the overall features of the reaction mechanism; however, mechanistic details remained unclear, specifically the following: (1) what is the energy barrier for formal C–H activation, (2) how does OAT take place, and (3) how to regenerate the

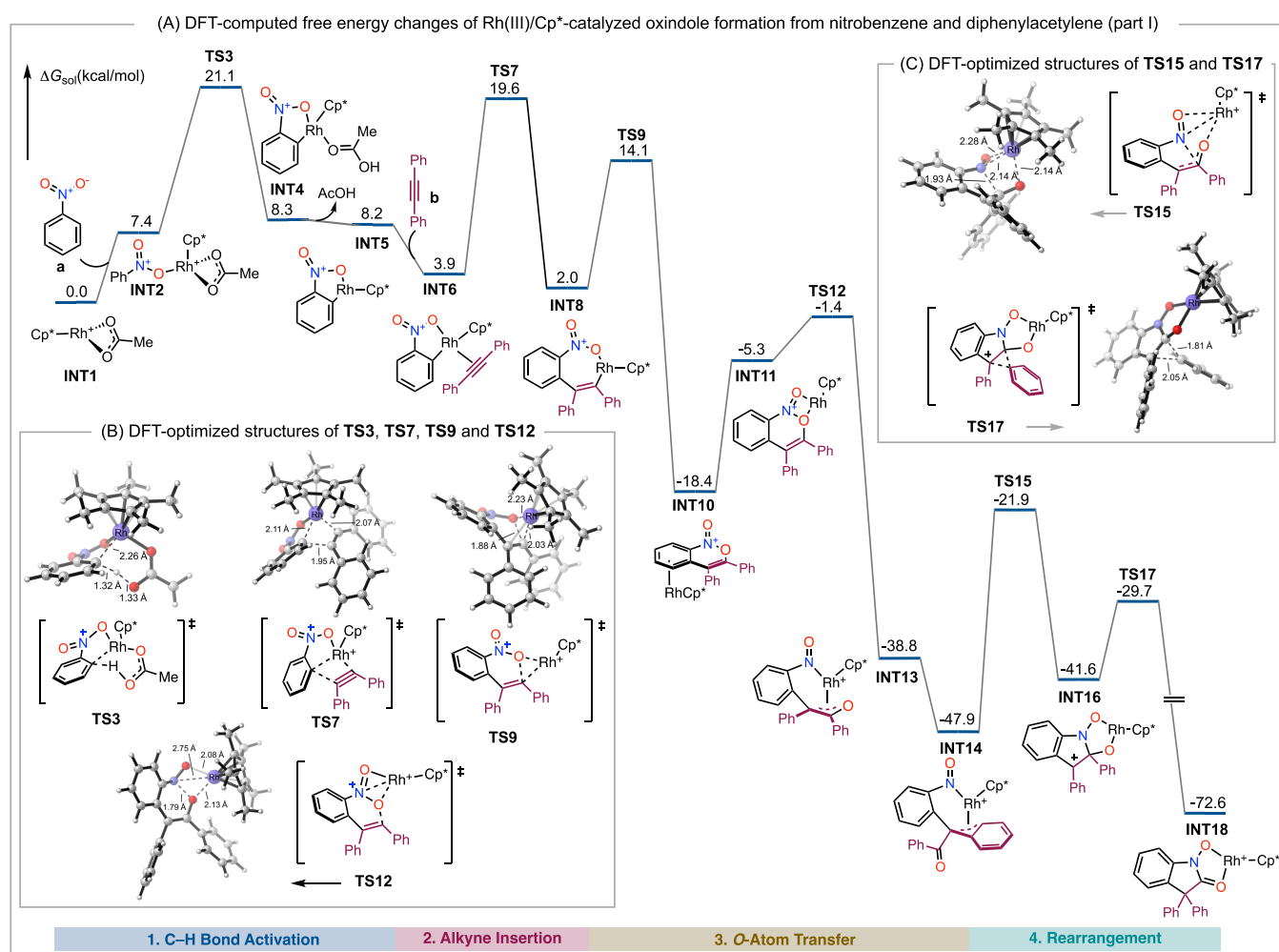


Figure 3. DFT-computed free energy changes (A) and DFT-optimized structures of selected transition states (B, C) of Rh(III)/Cp*-catalyzed oxindole formation from nitrobenzene and diphenylacetylene (part I).

active catalyst. To address these questions, a computational investigation of the reaction was undertaken at the PBE0-D3/def2-TZVPP-SMD(1,2-dichloroethane)//B3LYP-D3/def2-SVP-SMD(1,2-dichloroethane) level of theory.²⁴ The reaction between nitrobenzene and diphenylacetylene in the presence of acetic anhydride to afford product **1** using Cp*Rh(III) catalysts was used as the model reaction in the calculations. The free energy changes of the most favorable pathway of Rh(III)/Cp*-catalyzed oxindole formation are shown in Figures 3A and 4. Density functional theory (DFT)-optimized structures of selected transition states are shown in Figure 3B,C.

Starting from the catalytically active species INT1, which is generated from [Cp*RhCl₂]₂ and AgSbF₆ in the presence of Ac₂O by chloride abstraction by Ag⁺ and ligand exchange, nitrobenzene (a) coordination to the metal center occurs to form INT2. Subsequent CMD arises via TS3 to cleave the C-H bond, generating INT4. Acetic acid dissociation gives INT5. Then, with the association of alkyne **b**, a more stable species INT6 is produced from which alkyne insertion into the Rh-C bond takes place via TS7 to give seven-membered rhodacycle INT8. The alternative pathway involving alkyne insertion into the Rh-O bond is not feasible (Figure S27). Next, OAT affords the isolable η^3 -benzyl nitroso complex INT14, which was verified by NMR, HRMS, and X-ray studies. Our

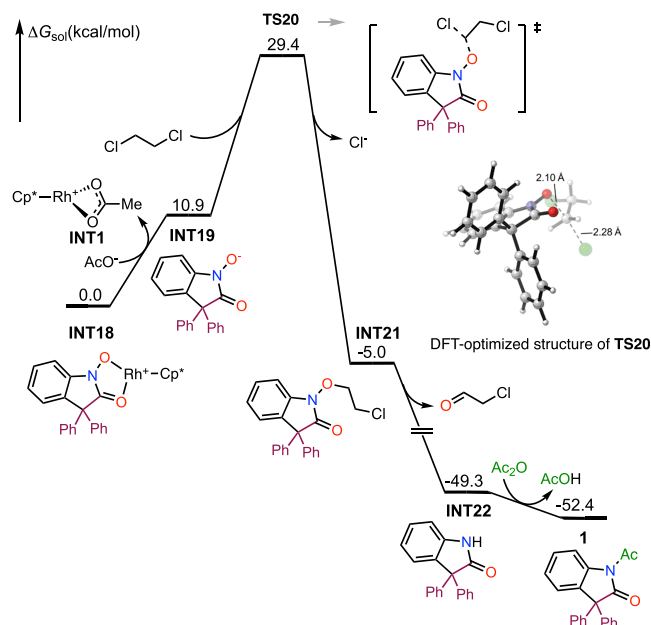


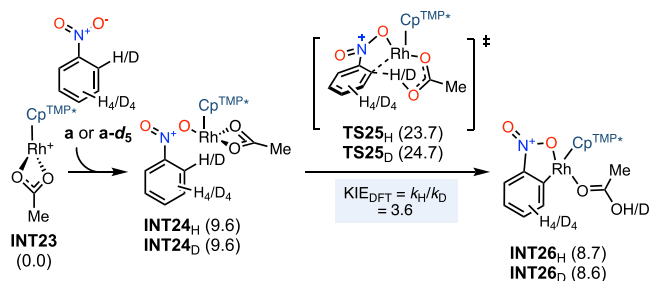
Figure 4. DFT-computed free energy changes of Rh(III)/Cp*-catalyzed oxindole formation from nitrobenzene and diphenylacetylene (part II).

computations indicate that this process proceeds through a reductive elimination (via **TS9**) affording the Rh(I) complex (**INT10**) followed by the oxidative addition of the N–O bond (via **TS12**) to generate the O-bond Rh(III)-enolate intermediate **INT13**. This intermediate adopts the C-enolate form (**INT14**) to give a more stable η^3 -benzyl coordination. Subsequent nucleophilic attack of the nitroso O on Rh via **TS15** leads to the formation of **INT16**. In analogy to the semipinacol rearrangement,²⁵ a 1,2-aryl shift via **TS17** affords the isolable N-oxido Rh(III) complex **INT18**. The helical shape of $\text{Cp}^{\text{TMP}*}$ might favor the nucleophilic attack since **39a** is converted into **40** at RT, while **39b** with disc-shaped Cp^* is stable.

Finally, based on **INT18**, ligand exchange with AcO^- regenerates the active catalytic species (**INT1**) for the next cycle, along with the formation of **INT19**. In the presence of 1,2-dichloroethane, we propose that a nucleophilic attack of **INT19** to 1,2-dichloroethane via **TS20** produces **INT21**.²⁶ Nucleophilic attack with the involvement of Rh is less favorable (Figure S28). After that, **INT21** evolves to acylated indolinone **1**²⁷ with the assistance of Ac_2O in a noncatalyzed pathway.²³

On the basis of the calculated free energy changes of the whole catalytic cycle (Figures 3 and 4), the rate-limiting step is C–H bond activation, and the overall energy barrier is 32.0 kcal/mol (21.1 kcal/mol (Figure 3, **INT1** to **TS3**) + 10.9 kcal/mol (Figure 4, **INT18** to **INT19**, corresponding to the energy required for the active catalyst (**INT1**) regeneration)). The calculated results are consistent with the experimental observations (Scheme 3). Moreover, the computed KIE at 120 °C using $\text{Cp}^{\text{TMP}*}\text{Rh}$ was 3.6, nearly reproducing the experimental results (Figure 2A, $\text{KIE}_{\text{exp}} = K_{\text{H}}/K_{\text{D}} = 3.5$).

Scheme 3. Computational KIE for the Rh-Catalyzed C–H Bond Activation of Nitrobenzenes **a** and **a-d₅**^a



^aFree energies are in kcal/mol at 120 °C.

Experimentally, $\text{Rh(III)/Cp}^{\text{TMP}*}$ performs better than Rh(III)/Cp^* , indicating that the former facilitates the occurrence of the rate-limiting step (C–H bond activation). To explore the origins of ligand-controlled reaction efficiency, we calculated the C–H bond activation step with the catalysis by $\text{Rh(III)/Cp}^{\text{TMP}*}$, and compared it to the same process with Rh(III)/Cp^* catalysis. As mentioned above, the overall energy barrier of C–H bond activation includes active catalyst regeneration (step 1) and CMD (step 2). For both cases, step 1 has very similar energetics (Figure S29), and the difference in reactivity arises from the second step (CMD step). As shown in Figure 5A, when employing $\text{Rh(III)/Cp}^{\text{TMP}*}$ as the catalyst, the barrier of C–H bond activation is lowered by 1.9 kcal/mol compared to the Rh(III)/Cp^* case (**TS25** vs. **TS3**), in agreement with the experimental results.

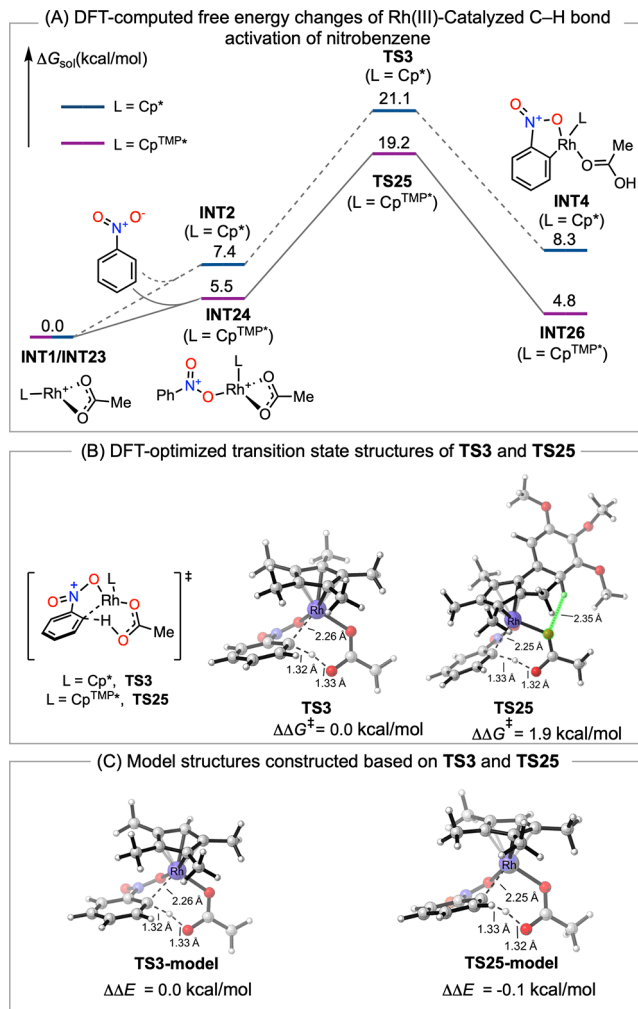


Figure 5. Comparison of C–H bond activation step with different catalysts.

After careful examination of the structures of **TS3** and **TS25**, we believe that the leading factor responsible for the energy difference is a hydrogen-bonding interaction, which is present in **TS25**, but absent in **TS3** (Figure 5B). To support our hypothesis, **TS3-model** and **TS25-model** were constructed by replacing methyl and aryl groups with hydrogens, respectively. After removing the hydrogen-bonding interaction from **TS25**, **TS3-model** and **TS25-model** have almost the same energy, in agreement with our hypothesis (Figure 5C).

CONCLUSIONS

In conclusion, we have developed a highly selective three-component protocol for the construction of oxindole derivatives with the formation of a quaternary center at the C3 position merely from nitroarenes and alkynes through Rh(III)-catalyzed one-pot cascade of C–H bond activation—OAT—[1,2]-aryl shift—deoxygenation—N-acylation. The reaction proceeds under redox-neutral conditions and tolerates a wide range of common functional groups. To improve the reactivity, we designed a new ligand, namely $\text{Cp}^{\text{TMP}*}$. Its resulting Rh(III) complex combines an electron-rich character required for C–H activation or OAT with a helicoidal shape to favor the C–H bond activation. The reaction pathway has been rationalized by capturing and fully analyzing three Rh(III) intermediates, and by a detailed exploration of the

mechanism with DFT calculations. This unique strategy generating nitrosoarenes from nitroarenes will pave the way to explore further their reactivities in the presence of other coupling partners in the quest for novel cascade transformations to expand the chemical space of *N*-heterocycles.

■ ASSOCIATED CONTENT

SI Supporting Information

The Supporting Information is available free of charge at <https://pubs.acs.org/doi/10.1021/jacs.2c10932>.

Experimental procedures, characterization data (1H and 13C NMR, HRMS, Fourier transform infrared) for all new compounds, and coordination geometries for DFT-optimized compounds (PDF)
FIDs for NMR data (ZIP)

Accession Codes

CCDC 2108500–2108504 and 2108506–2108507 contain the supplementary crystallographic data for this paper. These data can be obtained free of charge via www.ccdc.cam.ac.uk/data_request/cif, or by emailing data_request@ccdc.cam.ac.uk, or by contacting The Cambridge Crystallographic Data Centre, 12 Union Road, Cambridge CB2 1EZ, UK; fax: +44 1223 336033.

■ AUTHOR INFORMATION

Corresponding Authors

K. N. Houk – Department of Chemistry and Biochemistry, University of California, Los Angeles, Los Angeles, California 90095-1569, United States; orcid.org/0000-0002-8387-5261; Email: hok@chem.ucla.edu

Jean-François Soulé – Univ Rennes, CNRS UMR6226, Rennes F-3500, France; Present Address: Chimie ParisTech, PSL University, CNRS, Institute of Chemistry for Life and Health Sciences, 75005 Paris, France; orcid.org/0000-0002-6593-1995; Email: jean-francois.soule@chimieparistech.psl.eu

Authors

Marie Peng – Univ Rennes, CNRS UMR6226, Rennes F-3500, France

Chang-Sheng Wang – Univ Rennes, CNRS UMR6226, Rennes F-3500, France

Pan-Pan Chen – Department of Chemistry and Biochemistry, University of California, Los Angeles, Los Angeles, California 90095-1569, United States

Thierry Roisnel – Univ Rennes, CNRS UMR6226, Rennes F-3500, France

Henri Doucet – Univ Rennes, CNRS UMR6226, Rennes F-3500, France; orcid.org/0000-0002-1410-3663

Complete contact information is available at: <https://pubs.acs.org/doi/10.1021/jacs.2c10932>

Author Contributions

[§]M.P., C.-S.W., and P.-P.C. contributed equally to this paper.

Notes

The authors declare no competing financial interest.

■ ACKNOWLEDGMENTS

We thank Clement Orione (CRMPO) for NMR analysis and Jérôme Ollivier and Philippe Jehan (CRMPO) for the HRMS analysis. We are grateful to the National Science Foundation (CHE-1764328 to KNH) for financial support of this research,

and financial support from the Rennes 1 University (Ph.D. grant to M.P.), China Scholarship Council (Ph.D. grant to C.-S.W.), the Centre National de la Recherche Scientifique (CNRS) is also gratefully acknowledged. Calculations were performed on the IDRE Hoffman2 cluster at the University of California, Los Angeles, and the Extreme Science and Engineering Discovery Environment (XSEDE), which is supported by the National Science Foundation (OCI-1053575). We thank Umicore AG & Co. KG for their generous donation of rhodium(III) chloride hydrate.

■ REFERENCES

- (1) Heravi, M. M.; Zadsirjan, V. Prescribed Drugs Containing Nitrogen Heterocycles: an Overview. *RSC Adv.* **2020**, *10*, 44247–44311.
- (2) Chen, D.; Su, S.-J.; Cao, Y. Nitrogen Heterocycle-Containing Materials for Highly Efficient Phosphorescent OLEDs with Low Operating Voltage. *J. Mater. Chem. C* **2014**, *2*, 9565–9578.
- (3) (a) Stuart, D. R.; Bertrand-Laperle, M.; Burgess, K. M. N.; Fagnou, K. Indole Synthesis via Rhodium Catalyzed Oxidative Coupling of Acetanilides and Internal Alkynes. *J. Am. Chem. Soc.* **2008**, *130*, 16474–16475. (b) Stuart, D. R.; Alsabeh, P.; Kuhn, M.; Fagnou, K. Rhodium(III)-Catalyzed Arene and Alkene C–H Bond Functionalization Leading to Indoles and Pyrroles. *J. Am. Chem. Soc.* **2010**, *132*, 18326–18339. (c) Huestis, M. P.; Chan, L.; Stuart, D. R.; Fagnou, K. The Vinyl Moiety as a Handle for Regiocontrol in the Preparation of Unsymmetrical 2,3-Aliphatic-Substituted Indoles and Pyrroles. *Angew. Chem., Int. Ed.* **2011**, *50*, 1338–1341.
- (4) For selected examples on Rh(III)-catalyzed C–H bond annulation, see: (a) Su, Y.; Zhao, M.; Han, K.; Song, G.; Li, X. Synthesis of 2-Pyridones and Iminoesters via Rh(III)-Catalyzed Oxidative Coupling between Acrylamides and Alkynes. *Org. Lett.* **2010**, *12*, 5462–5465. (b) Wang, C.; Sun, H.; Fang, Y.; Huang, Y. General and Efficient Synthesis of Indoles through Triazene-Directed C–H Annulation. *Angew. Chem., Int. Ed.* **2013**, *52*, 5795–5798. (c) Zhao, D.; Shi, Z.; Glorius, F. Indole Synthesis by Rhodium(III)-Catalyzed Hydrazine-Directed C–H Activation: Redox-Neutral and Traceless by N–N Bond Cleavage. *Angew. Chem., Int. Ed.* **2013**, *52*, 12426–12429. (d) Liu, B.; Song, C.; Sun, C.; Zhou, S.; Zhu, J. Rhodium(III)-Catalyzed Indole Synthesis Using N–N Bond as an Internal Oxidant. *J. Am. Chem. Soc.* **2013**, *135*, 16625–16631. (e) Yang, Y.; Wang, X.; Li, Y.; Zhou, B. A [4+1] Cyclative Capture Approach to 3H-Indole-N-oxides at Room Temperature by Rhodium(III)-Catalyzed C–H Activation. *Angew. Chem., Int. Ed.* **2015**, *54*, 15400–15404. (f) Li, X.; Li, X.; Jiao, N. Rh-Catalyzed Construction of Quinolin-2(1H)-ones via C–H Bond Activation of Simple Anilines with CO and Alkynes. *J. Am. Chem. Soc.* **2015**, *137*, 9246–9249. (g) Font, M.; Cendón, B.; Seoane, A.; Mascareñas, J. L.; Gullías, M. Rhodium(III)-Catalyzed Annulation of 2-Alkenyl Anilides with Alkynes through C–H Activation: Direct Access to 2-Substituted Indolines. *Angew. Chem., Int. Ed.* **2018**, *57*, 8255–8259. (h) Özkaya, B.; Bub, C. L.; Patureau, F. W. Step and Redox Efficient Nitroarene to Indole Synthesis. *Chem. Commun.* **2020**, *56*, 13185–13188. (i) Singh, A.; Shukla, R. K.; Volla, C. M. R. Rh(III)-Catalyzed [5 + 1] Annulation of 2-Alkenylanilides and 2-Alkenylphenols with Allenyl Acetates. *Chem. Sci.* **2022**, *13*, 2043–2049.
- (5) Zhang, X.; Qi, Z.; Li, X. Rhodium(III)-Catalyzed C–C and C–O Coupling of Quinoline N-Oxides with Alkynes: Combination of C–H Activation with O-Atom Transfer. *Angew. Chem., Int. Ed.* **2014**, *53*, 10794–10798.
- (6) Dateer, R. B.; Chang, S. Selective Cyclization of Arylnitrones to Indolines under External Oxidant-Free Conditions: Dual Role of Rh(III) Catalyst in the C–H Activation and Oxygen Atom Transfer. *J. Am. Chem. Soc.* **2015**, *137*, 4908–4911.
- (7) Yan, H.; Wang, H.; Li, X.; Xin, X.; Wang, C.; Wan, B. Rhodium-Catalyzed C–H Annulation of Nitrones with Alkynes: A Regiospecific Route to Unsymmetrical 2,3-Diaryl-Substituted Indoles. *Angew. Chem., Int. Ed.* **2015**, *54*, 10613–10617.

- (8) (a) Li, B.; Xu, H.; Wang, H.; Wang, B. Rhodium-Catalyzed Annulation of Tertiary Aniline *N*-Oxides to *N*-Alkylindoles: Regioselective C–H Activation, Oxygen-Atom Transfer, and *N*-Dealkylative Cyclization. *ACS Catal.* **2016**, *6*, 3856–3862. (b) Huang, X.; Liang, W.; Shi, Y.; You, J. Rh(III)-Catalyzed Chemoselective C–H Functionalizations of Tertiary Aniline *N*-Oxides with Alkynes. *Chem. Commun.* **2016**, *52*, 6253–6256.
- (9) Palav, A.; Misal, B.; Ernolla, A.; Parab, V.; Waske, P.; Khandekar, D.; Chaudhary, V.; Chaturbhuj, G. The *m*-CPBA–NH₃(g) System: A Safe and Scalable Alternative for the Manufacture of (Substituted) Pyridine and Quinoline *N*-Oxides. *Org. Process Res. Dev.* **2019**, *23*, 244–251.
- (10) (a) Greish, A. Nitration of Aromatic Hydrocarbons over Heterogenous Catalysts. *Rus. Chem. J.* **2004**, *48*, 92–104. (b) Yan, G.; Yang, M. Recent Advances in the Synthesis of Aromatic Nitro Compounds. *Org. Biomol. Chem.* **2013**, *11*, 2554–2566. (c) Koskin, A. P.; Mishakov, I. V.; Vedyagin, A. A. In search of Efficient Catalysts and Appropriate Reaction Conditions for Gas Phase Nitration of Benzene. *Resour. Technol.* **2016**, *2*, 118–125. (d) Calvo, R.; Zhang, K.; Passera, A.; Katayev, D. Facile Access to Nitroarenes and Nitroheteroarenes using *N*-Nitrosaccharin. *Nat. Commun.* **2019**, *10*, 3410.
- (11) (a) Caron, L.; Campeau, L.-C.; Fagnou, K. Palladium-Catalyzed Direct Arylation of Nitro-Substituted Aromatics with Aryl Halides. *Org. Lett.* **2008**, *10*, 4533–4536. (b) Yi, Z.; Aschenaki, Y.; Daley, R.; Davick, S.; Schnaith, A.; Wander, R.; Kalyani, D. Palladium Catalyzed Arylation and Benzylolation of Nitroarenes Using Aryl Sulfonates and Benzyl Acetates. *J. Org. Chem.* **2017**, *82*, 6946–6957. (c) Tan, E.; Montesinos-Magraner, M.; García-Morales, C.; Mayans, J. G.; Echavarren, A. M. Rhodium-Catalyzed *Ortho*-Alkynylation of Nitroarenes. *Chem. Sci.* **2021**, *12*, 14731–14739.
- (12) For selected examples of formation and reactivities of nitrosoarenes, see: (a) Jana, N.; Zhou, F.; Driver, T. G. Promoting Reductive Tandem Reactions of Nitrostyrenes with Mo(CO)₆ and a Palladium Catalyst To Produce 3H-Indoles. *J. Am. Chem. Soc.* **2015**, *137*, 6738–6741. (b) Shevlin, M.; Guan, X.; Driver, T. G. Iron-Catalyzed Reductive Cyclization of *o*-Nitrostyrenes Using Phenylsilane as the Terminal Reductant. *ACS Catal.* **2017**, *7*, 5518–5522. (c) Zhou, F.; Wang, D.-S.; Guan, X.; Driver, T. G. Nitroarenes as the Nitrogen Source in Intermolecular Palladium-Catalyzed Aryl C–H Bond Aminocarbonylation Reactions. *Angew. Chem., Int. Ed.* **2017**, *56*, 4530–4534. (d) Ford, R. L.; Alt, I.; Jana, N.; Driver, T. G. Intramolecular Pd-Catalyzed Reductive Amination of Enolizable sp³ C–H Bonds. *Org. Lett.* **2019**, *21*, 8827–8831. (e) Shimizu, H.; Yoshinaga, K.; Yokoshima, S. Nitron Formation by Reaction of an Enolate with a Nitro Group. *Org. Lett.* **2021**, *23*, 2704–2709.
- (13) For selected examples to prepare oxindoles, see: (a) Overman, L. E.; Poon, D. J. Asymmetric Heck Reactions via Neutral Intermediates: Enhanced Enantioselectivity with Halide Additives Gives Mechanistic Insights. *Angew. Chem., Int. Ed.* **1997**, *36*, 518–521. (b) Ashimori, A.; Bachand, B.; Calter, M. A.; Govek, S. P.; Overman, L. E.; Poon, D. J. Catalytic Asymmetric Synthesis of Quaternary Carbon Centers. Exploratory Studies of Intramolecular Heck Reactions of (*Z*)- α,β -Unsaturated Anilides and Mechanistic Investigations of Asymmetric Heck Reactions Proceeding via Neutral Intermediates. *J. Am. Chem. Soc.* **1998**, *120*, 6488–6499. (c) Marti, C.; Carreira, E. M. Construction of Spiro[pyrrolidine-3,3'-oxindoles] – Recent Applications to the Synthesis of Oxindole Alkaloids. *Eur. J. Org. Chem.* **2003**, *2003*, 2209–2219. (d) Galliford, C. V.; Scheidt, K. A. Pyrrolidinyl-Spirooxindole Natural Products as Inspirations for the Development of Potential Therapeutic Agents. *Angew. Chem., Int. Ed.* **2007**, *46*, 8748–8758. (e) Duguet, N.; Slawin, A. M. Z.; Smith, A. D. An Asymmetric Hetero-Claisen Approach to 3-Alkyl-3-aryloxindoles. *Org. Lett.* **2009**, *11*, 3858–3861. (f) Çelebi-Ölçüm, N.; Lam, Y. H.; Richmond, E.; Ling, K. B.; Smith, A. D.; Houk, K. N. Pericyclic Cascade with Chirality Transfer: Reaction Pathway and Origin of Enantioselectivity of the Hetero-Claisen Approach to Oxindoles. *Angew. Chem., Int. Ed.* **2011**, *50*, 11478–11482.
- (14) See [Supporting Information](#) for more details.
- (15) Piou, T.; Romanov-Michailidis, F.; Romanova-Michaelides, M.; Jackson, K. E.; Semakul, N.; Taggart, T. D.; Newell, B. S.; Rithner, C. D.; Paton, R. S.; Rovis, T. Correlating Reactivity and Selectivity to Cyclopentadienyl Ligand Properties in Rh(III)-Catalyzed C–H Activation Reactions: An Experimental and Computational Study. *J. Am. Chem. Soc.* **2017**, *139*, 1296–1310.
- (16) Shibata, Y.; Tanaka, K. Catalytic [2+2+1] Cross-Cyclo-trimerization of Silylacetylenes and Two Alkynyl Esters To Produce Substituted Silylfulvenes. *Angew. Chem., Int. Ed.* **2011**, *50*, 10917–10921.
- (17) Wodrich, M. D.; Ye, B.; Gonthier, J. F.; Corminboeuf, C.; Cramer, N. Ligand-Controlled Regiodivergent Pathways of Rhodium-(III)-Catalyzed Dihydroisoquinolone Synthesis: Experimental and Computational Studies of Different Cyclopentadienyl Ligands. *Chem. – Eur. J.* **2014**, *20*, 15409–15418.
- (18) The electronic properties can be estimated from the redox potentials of Rh complexes.
- (19) For the F effect in C–H bond functionalization, see: (a) Lafrance, M.; Rowley, C. N.; Woo, T. K.; Fagnou, K. Catalytic Intermolecular Direct Arylation of Perfluorobenzenes. *J. Am. Chem. Soc.* **2006**, *128*, 8754–8756. (b) Yan, T.; Zhao, L.; He, M.; Soulé, J.-F.; Bruneau, C.; Doucet, H. Reactivity of 3-Substituted Fluorobenzenes in Palladium-Catalyzed Direct Arylations with Aryl Bromides. *Adv. Synth. Catal.* **2014**, *356*, 1586–1596. (c) He, M.; Soulé, J.-F.; Doucet, H. Reactivity of *Para*-Substituted Fluorobenzenes in Palladium-catalyzed Intermolecular Direct Arylations. *ChemCatChem* **2015**, *7*, 2130–2140. (d) Obligacion, J. V.; Bezdek, M. J.; Chirik, P. J. C(sp²)–H Borylation of Fluorinated Arenes Using an Air-Stable Cobalt Precatalyst: Electronically Enhanced Site Selectivity Enables Synthetic Opportunities. *J. Am. Chem. Soc.* **2017**, *139*, 2825–2832. (e) Boyaala, R.; Touzani, R.; Roisnel, T.; Dorcet, V.; Caytan, E.; Jacquemin, D.; Boixel, J.; Guerschais, V.; Doucet, H.; Soulé, J.-F. Catalyst-Controlled Regiodivergent C–H Arylation Site of Fluorinated 2-Arylpyridine Derivatives: Application to Luminescent Iridium(III) Complexes. *ACS Catal.* **2019**, *9*, 1320–1328.
- (20) (a) Bariwal, J.; Voskressensky, L. G.; Van der Eycken, E. V. Recent Advances in Spirocyclization of Indole Derivatives. *Chem. Soc. Rev.* **2018**, *47*, 3831–3848. (b) Pradhan, S.; De, P. B.; Shah, T. A.; Punniyamurthy, T. Recent Advances in Metal-catalyzed Alkylation, Alkenylation and Alkynylation of Indole/indoline Benzenoid Nucleus. *Chem. – Asian J.* **2020**, *15*, 4184–4198.
- (21) Control experiments using other reduced intermediates of nitrobenzene (i.e., aniline, *N*-hydroxybenzenamine, nitrosobenzene, azoxybenzene, or azobenzene) did not lead the cascade reaction, see [Supporting Information](#) for more details.
- (22) Vicente, J.; Abad, J. A.; Lahoz, F. J.; Plou, F. J. Synthesis, Reactivity, and X-Ray Crystal Structure of [Rh{C₆H₄N(O)O₂}(η -C₅Me₅)Cl]. *J. Chem. Soc., Dalton Trans.* **1990**, 1459–1462.
- (23) Lee, B. H.; Biswas, A.; Miller, M. J. [1,2]-Anionic Rearrangements of Substituted *N*-Hydroxy-2-azetidinones and Applications to the Synthesis of Bicyclic Beta-Lactams. *J. Org. Chem.* **1986**, *51*, 106–109.
- (24) Computational details are included in the [Supporting Information](#).
- (25) Delayre, B.; Wang, Q.; Zhu, J. Natural Product Synthesis Enabled by Domino Processes Incorporating a 1,2-Rearrangement Step. *ACS Cent. Sci.* **2021**, *7*, 559–569.
- (26) For previous examples of a participating role of 1,2-dichloroethane in Rh(III)-catalyzed C–H functionalization, see: (a) Wang, Z.; Yin, J.; Zhou, F.; Liu, Y.; You, J. Multicomponent Reactions of Pyridines To Give Ring-Fused Pyridiniums: In Situ Activation Strategy Using 1,2-Dichloroethane as a Vinyl Equivalent. *Angew. Chem., Int. Ed.* **2019**, *58*, 254–258. (b) Hu, W.; Yan, L.; Zuo, Y.; Kong, S.; Pu, Y.; Tang, Q.; Wang, X.; He, X.; Shang, Y. Rhodium(III)-Catalyzed Three-Component Cascade Annulation for Modular Assembly of *N*-Alkoxyated Isoindolin-1-Ones with Quaternary Carbon Center. *Adv. Synth. Catal.* **2022**, *364*, 2589–2595.

(27) We computationally investigated the possibility of coordination of the product (**1**) with the catalyst, and details are included in the [Supporting Information](#).